

A Journal of the Gesellschaft Deutscher Chemiker

Angewandte Chemie

GDCh

International Edition

www.angewandte.org

Accepted Article

Title: Light-Driven Reversible Multicolor Supramolecular Shuttle

Authors: Rong Zhang, Yong Chen, and Yu Liu

This manuscript has been accepted after peer review and appears as an Accepted Article online prior to editing, proofing, and formal publication of the final Version of Record (VoR). The VoR will be published online in Early View as soon as possible and may be different to this Accepted Article as a result of editing. Readers should obtain the VoR from the journal website shown below when it is published to ensure accuracy of information. The authors are responsible for the content of this Accepted Article.

To be cited as: *Angew. Chem. Int. Ed.* **2023**, e202315749

Link to VoR: <https://doi.org/10.1002/anie.202315749>

Light-Driven Reversible Multicolor Supramolecular Shuttle

Rong Zhang,^[a] Yong Chen,^[a] Yu Liu*^[a,b,c]

[a] R. Zhang, Prof. Y. Chen, Prof. Y. Liu
College of Chemistry, State Key Laboratory of Elemento-Organic Chemistry, Nankai University
Tianjin 300071 (P. R. China)
E-mail: yuliu@nankai.edu.cn

[b] Prof. Y. Liu
Collaborative Innovation Center of Chemical Science and Engineering (Tianjin), Nankai University
Tianjin 300071 (P. R. China)

[c] Prof. Y. Liu
Haihe Laboratory of Sustainable Chemical Transformations
Tianjin 300071 (P. R. China)

Supporting information for this article is given via a link at the end of the document.

Abstract: Light-driven multicolor supramolecular systems mainly rely on doping dyes or photo-reaction to produce unidirectional luminescence. Herein, we use visible light to drive the bidirectional reversible multicolor supramolecular shuttle from blue to green, white, yellow, up to orange via simple encapsulation of spiropyran-modified cyanostilbene (BCNMC) by macrocycle cucurbit[8]uril (CB[8]) monomer. The resultant host-guest complex presented effectively enhanced fluorescence properties, i.e. the multicolor fluorescence shuttle changed from blue to orange in dark in 2 hours and reverted to the original state upon visible light irradiation for 30 s. Benefiting from the sensitivity of spiropyran to light, it can spontaneously isomerize from the ring-opened state to a ring-closed isomer in aqueous solution, and this photo-isomerization reaction achieves a reversible process under visible light irradiation, leading to the multicolor luminescence supramolecular shuttle due to the intramolecular energy transfer. In addition, the light also drove the reversible conversion of the topological morphology of the host-guest complex from two-dimensional nanoplatelets to nanospheres. Different from the widely reported molecular rotaxane “shuttle”, the macrocyclic host CB[8] confined guest spiropyran supramolecular shuttle not only modulated reversible topological morphology by light but also exhibited multicolor luminescence, which was successfully applied in programmed and rewritable information encryption.

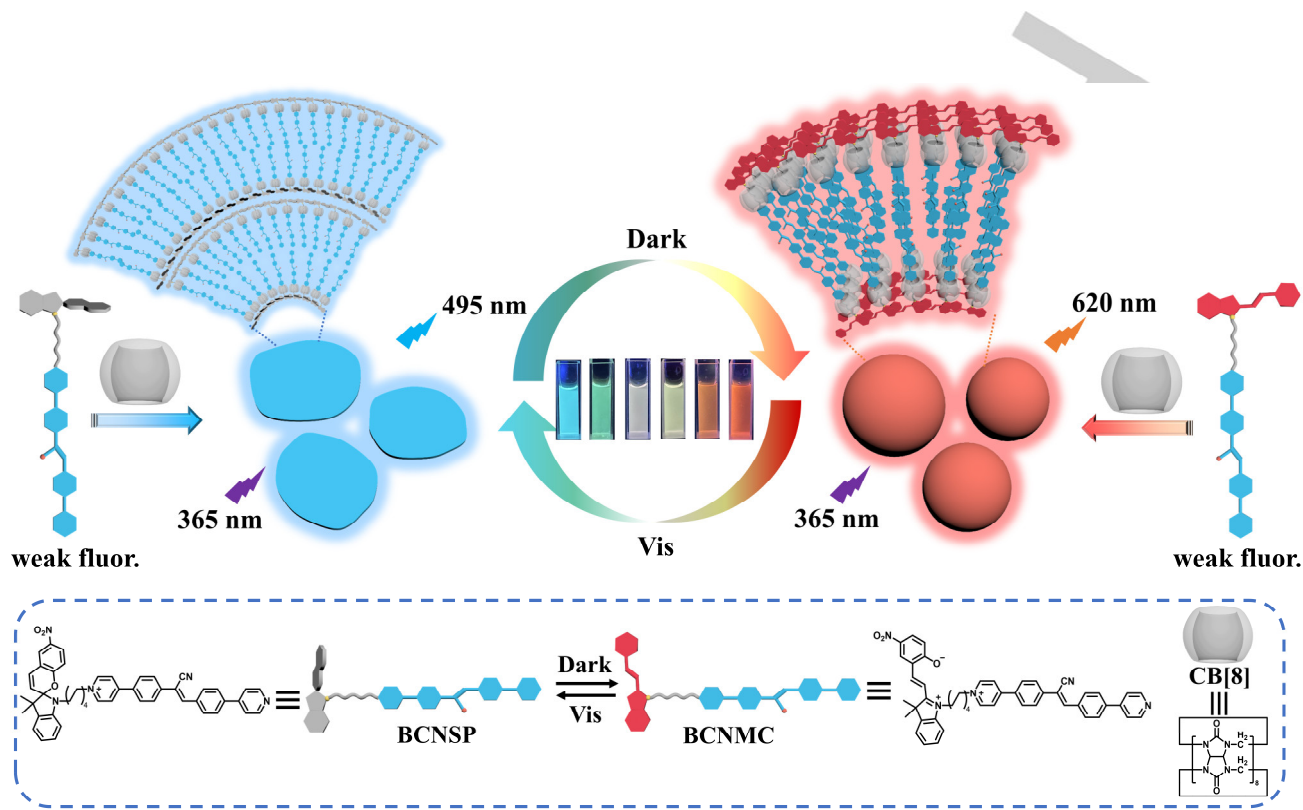
Dynamically tunable luminescent systems generally exhibited sensitive modulation of luminescence performance under a variety of external stimuli, such as light, temperature, magnetism, mechanical force, chemicals, electric field, and pH, thus have drawn considerable attention and demonstrated a wide range of applications in the fields of information encryption, bioimaging, probing, sensing, diagnosis and therapeutics.^[1] Among the various stimulus-response modulation strategies, the light-driven reaction and conversion of topological morphology have been widely investigated in scientific research due to their advantages of cleanliness, controllability, noninvasive, high sensitivity and super temporal-spatial resolution.^[2] Recently, non-covalent supramolecular strategies have been employed by many researchers to construct photo-responsive luminescent systems, which were simpler and easier to manipulate than the conventional approaches, and were also beneficial in enhancing the luminescence intensity and sensitivity with light signal.^[3] Most of the reported photo-responsive supramolecular luminescence systems have been constructed based on several types of traditional photo-responsive molecular skeletons including diaryliethene, spiropyran and azobenzene, etc.^[4] For example, Park and coworkers designed a color-specific

photoswitching, which combined a blue fluorescent diarylethene and an orange fluorescent organic dye to fabricate the two-component dual-emissive system into biocompatible polymer nanoparticles, and the color-specific photoswitching was successfully observed in cells.^[5] Li and coworkers reported photo-activated supramolecular dissipative system that are composed of zwitterionic sulfonato-spiropyran and polyethyleneimine. After loading different dyes, the supramolecular dissipative system exhibited multiple fluorescent colors of the dyes themselves and their mixture, which had been successfully applied in self-erasing anti-counterfeiting with time-dependent properties.^[6] We also reported a multicolor luminescence ternary supramolecular system based on diarylethene derivatives, carbon dots and cucurbit[8]uril (CB[8]), which was observed to emit multicolor luminescence including pure white light emission under UV illumination thanks to the photo-switching properties of diarylethene.^[7] The unidirectional control of emissive supramolecular system is generally achieved by excitation wavelength-dependent photoluminescence, cascade energy transferring of doping dyes, and multicomponent photochemical reactions.^[8] However, bidirectionally reversible multicolor luminescence shuttle has not been reported yet in the field of molecular machines, despite rotaxane-like molecular machines having been created for several decades. Constructing light-driven bidirectional multicolor luminescent shuttle by taking advantage of simple supramolecular system strategies between macrocyclic host and guest is still rare, to the best of knowledge, especially spiropyran photo-switchable molecule skeletons supramolecular system due to its weak fluorescence emission intensity and low quantum yield.

Herein, we reported a multicolor reversible supramolecular shuttle composed of spiropyran-modified cyanostilbene derivative (BCNMC) and CB[8] (Scheme 1). The guest BCNMC encapsulated in the CB[8] cavity produced a significantly enhanced fluorescence intensity at 495 nm. During subsequent placement in dark, the spiropyran moiety was gradually isomerized from the ring-closed state to the ring-opened state whose energy matched that of the cyanostilbene moiety, thus enabling intramolecular energy transfer and leading to the transition from the initial blue fluorescence at 495 nm to the fluorescence at 620 nm. The fluorescence color change could be reversibly reversed to the initial blue fluorescence again upon visible light irradiation. As a result, supramolecular systems with reversible multicolor luminescence including blue, green, white, yellow, and orange were successfully constructed. Surprisingly, the supramolecular system not only modulated the fluorescence color change under alternating visible light irradiation and

darkness, but also simultaneously regulated the topological morphology of the host-guest complex between nanoplatelets and nanospheres. Finally, the multicolor reversible

supramolecular shuttle was successfully applied in rewritable anti-counterfeiting.



Scheme 1. Schematic illustration of the construction and modulation of multicolor reversible supramolecular shuttle $\text{BCNMC} \subset \text{CB}[8]$.

The ring-closed spiropyran-modified cyanostilbene derivative (BCNSP) was synthesized by a substitution reaction between 4-(4-(cyanomethyl)phenyl)pyridine and spiropyran derivative (Scheme S1), and the detailed characterizations for BCNSP and reference compound cyanostilbene modified by alkyl chain (BCN4C) including ^1H NMR, ^{13}C NMR, and HR-MS were supplied in Figures S1-S4. Modification of spiropyran on cyanostilbene moiety was designed to endow the guest molecule with good photo-responsiveness by bridging the distance between the two backbones. In order to investigate whether the guest retained excellent photo-responsiveness, UV-vis spectroscopy was used to monitor the change in absorption of the guest under different light conditions. The experimental results of the aqueous solution of the guest after being left for 120 min protected from light showed a characteristic absorption peak at 370 nm and a broad absorption peak centered at 510 nm, which was attributed to the ring-opened form of BCNMC (Figure 1a). Immediately after the solution was irradiated by visible light, the absorption peak at 510 nm gradually weakened and disappeared after 30 s of the irradiation, which was caused by the isomerization of the spiropyran moiety into a ring-closed form BCNSP induced by visible light irradiation. Using alternating visible light irradiation and darkness, the absorption peak at 510 nm in UV-vis spectra was reversibly switched, which could be reversibly cycled more than five times without significant fatigue (Figure S5). The configuration inversion between BCNMC and BCNSP was further

investigated by ^1H NMR spectroscopy (Figure 1b), which revealed that BCNMC was efficiently inverted to BCNSP when irradiated by visible light. In addition, a calibration curve was established by the changes in the UV-vis absorption spectra of BCNMC at increasing concentrations to investigate the conversion efficiency between BCNMC and BCNSP (Figure S6). Ring-opened BCNMC reverted to ring-closed BCNSP upon visible light irradiation for 30 s and then 89.4% of the original BCNMC recovered over 120 min in dark owing to thermal relaxation (Figure 1c). At the same time, the obvious solution color change from pink to colorless was observed by the naked eye during visible light irradiation. All these results demonstrated the good tunable photophysical characteristics of the guest.

It is well known that the macrocyclic host cucurbituril is able to effectively encapsulate positively charged guest molecules and enhance the photoluminescence of the guest.^[9] Therefore, the host-guest binding behaviors of CB[8] cavities to the ring-opened form of BCNMC with positive charges was studied by UV-vis spectroscopy under dark condition. A bathochromic shift of the major absorption peak at 370 nm was observed as the concentration of CB[8] in the host-guest mixture solution gradually increasing, and the characteristic absorption peak slowly increased and stabilized when the concentrations of CB[8] and BCNMC were equal. (Figure 1d). The association constant (K_a) of $\text{BCNMC} \subset \text{CB}[8]$ complex was determined as $7.21 \times 10^6 \text{ M}^{-1}$ by the corresponding nonlinear least-squares fitting formula (Figure S7).

Moreover, the 1:1 bonding ratio between CB[8] and BCNMC was also confirmed based on the maximum value at a molar fraction of 0.5 according to the Job's plot (Figure S8). In addition, ^1H NMR signals of bridged alkyl chains protons were broadened and underwent an upfield shift in the presence of CB[8] (Figure S9), indicating that the CB[8] should be mainly encapsulated in the bridged alkyl chains. Moreover, the UV-vis titration experiment and Job's plot were employed to explore the binding behaviors between CB[8] and the ring-closed form of BCNSP after visible irradiation for 30 s. Similarly, the gradual increased concentration of CB[8] in the mixed host-guest solution resulted in a redshift and enhancement of the absorption peak at 370 nm according to the UV-vis spectra (Figure S10). The association constant (K_a) was calculated to be $1.02 \times 10^7 \text{ M}^{-1}$, and Job's plot reflected the 1:1 binding stoichiometry between BCNSP and CB[8], which was consistent with the bonding mode of the ring-opened form of BCNMC and CB[8] (Figure S11). These results showed that CB[8] could stably encapsulate the guest whether the guest was a ring-opened form of BCNMC or a ring-closed isomer.

Furthermore, the photo-responsive properties of the BCNMC \subset CB[8] host-guest complex were explored by UV-vis spectroscopy. Under sustained visible light irradiation, the absorption peak at 510 nm attributed to the spiropyran unit shown in Figure S12 regularly decreased and tended to disappear within 30 s, revealing the conversion from BCNMC to its photo-isomeric products. Comparatively, the absorption band centered at 510 nm was almost completely back to its original intensity as the subsequent placement in dark for 120 min (Figure S13). The change in UV-vis absorption of the host-guest complexes was consistent with that of the free guest, which was resulting from the reverse isomerization from ring-closed conformation to ring-opened one. Notably, the cycles between the appearance and disappearance of the absorption peaks performed at least five times with great fatigue resistance. Interestingly, the inclusion complex of CB[8] still retained the good photo-responsiveness of the guest. Transmission electron microscope (TEM) was used to investigate the morphology conversion of the host-guest complex in solution (Figure 1e-1g). Interestingly, different from the amorphous morphology with a small size of free guests (Figure S14), TEM images of host-guest complex BCNSP \subset CB[8] showed numerous dispersive nanoplatelets while BCNMC \subset CB[8] formed larger-sized nanospheres with a particle size of about 500 nm, and BCNMC \subset CB[8] reversed to the original nanoplatelets after visible light irradiation for 30 s. The average diameter was measured as 357 nm for BCNSP \subset CB[8] and 437 nm for BCNMC \subset CB[8] via dynamic light scattering (DLS), which were consistent with the TEM results (Figure S15).

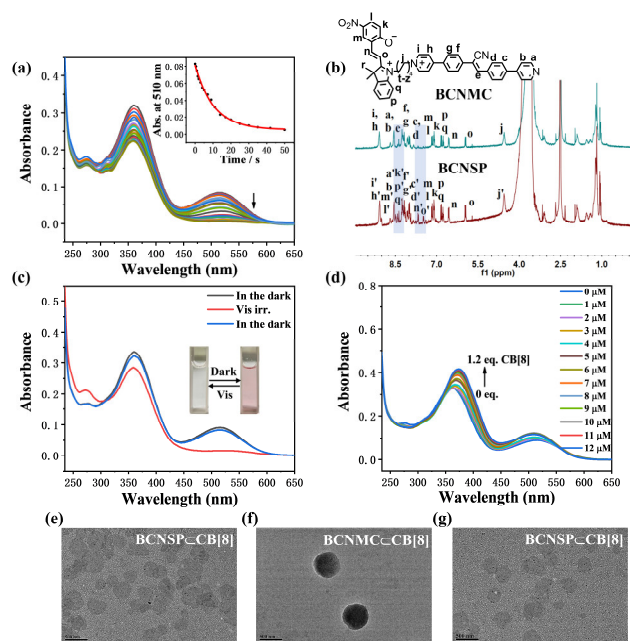


Figure 1. (a) UV-vis spectroscopy of BCNMC at different times of visible light irradiation and plot of the intensity of the absorption peak at 510 nm versus time (inset). (b) ^1H NMR spectroscopy of BCNSP after visible light irradiation for 30 s and BCNMC after light avoidance for 120 min (400 MHz, DMSO- d_6 , 25 $^\circ\text{C}$). (c) UV-Vis spectroscopy of BCNMC, BCNSP and recovered BCNMC after one cycle of visible light irradiation and darkness. (d) UV-vis spectroscopy of BCNMC with the addition of CB[8] ([BCNMC] = $1.0 \times 10^{-5} \text{ M}$, [CB[8]] = $0-1.2 \times 10^{-5} \text{ M}$). (e) TEM image of BCNSP \subset CB[8] and (f) BCNMC \subset CB[8] and (g) BCNSP \subset CB[8] after one cycle ([BCNMC] = $1.0 \times 10^{-5} \text{ M}$, [CB[8]] = $1.0 \times 10^{-5} \text{ M}$).

It has been reported that cyanostilbene derivative has good aggregation-induced luminescence properties,^[10] however, both ring-closed isomer BCNSP and ring-opened isomer BCNMC only exhibited weak fluorescence that was barely observed by the naked eye (Figure S16), which should be due to the influence of modified spiropyran moiety. Surprisingly, as the concentration of CB[8] gradually increased in the host-guest complex solution, the fluorescence intensity at 495 nm assigned to the cyanostilbene moiety under visible light irradiation enhanced more than 8 times compared to free BCNSP (Figure 2a), which was attributed to not only the movement of the guest from the polar aqueous solution to the non-polar macrocyclic cavity, but also the macrocyclic-confinement of CB[8] synergistically enhancing the luminescence of the cyanostilbene moiety.^[11] And the enhancement of the blue fluorescence was accomplished almost instantly with the addition of CB[8] (Figure S17). In contrast, BCNMC kept in dark for 120 min showed two emission peaks at 495 nm and 620 nm, respectively. Both fluorescence peaks were equally enhanced by gradually increasing the proportion of CB[8] in the solution under light-avoidance conditions (Figure S18). The photoluminescence mapping spectra showed that ring-opened BCNMC \subset CB[8] had fluorescence emission at about 500 nm and 600 nm after being placed in dark (Figure S19). Relatively, ring-closed BCNSP \subset CB[8] host-guest complex that was induced by the visible light irradiation caused the fluorescence emission at 600 nm to almost disappear, which was completely dominated by the emission at 500 nm. Light-regulated fluorescence change of the supramolecular system was monitored by fluorescence spectra to

investigate the photo-responsive behaviors. The fluorescence emission of BCNSP \subset CB[8] at 495 nm gradually quenched with prolonging the time of placement in dark upon excitation at 365 nm as shown in the photoluminescence spectra, accompanied by a gradual increase of fluorescence emission attributed to BCNMC \subset CB[8] at 620 nm (Figure 2b). When the BCNMC \subset CB[8] aqueous solution was exposed to visible light irradiation, the fluorescence emission was completely reversed (Figure S20), thus enabling reversible multicolor luminescence. The reversible change of fluorescence emission could be cycled more than five times without significant fatigue by alternating visible light irradiation and standing in dark (Figure 2c, 2d and S21). Moreover, the fluorescent color change from blue to orange that was apparent under UV lamp (365 nm) could also be captured by the naked eye and portable camera (Figure 2e). The reverse fluorescence color change from orange to blue was then achieved during visible light irradiation. The direction of the fluorescence color change was similarly corroborated in the 1931 CIE chromaticity diagram, which was depicted from (0.256, 0.389) to (0.399, 0.391) with progressive dark treatment and visible light irradiation (Figure 2f). Furthermore, the fluorescence lifetime of the supramolecular system at different states at 495 nm was measured according to the time-resolved photoluminescence curves, which indicated the lifetime of 7.06 ns and 7.21 ns for this emission peak of BCNMC \subset CB[8] and BCNSP \subset CB[8] respectively, which were similar to the lifetimes of the free guest BCNMC (7.11 ns) and BCNSP (6.93 ns) (Figure S22). Additionally, the quantum yield results show that BCNSP \subset CB[8] had a quantum yield of 6.24%, which was significantly higher than that of the individual BCNSP (0.05%). Similarly, the quantum yield of BCNMC \subset CB[8] reached 4.54% compared to BCNMC (0.02%), indicating CB[8] encapsulation of the guest efficiently enhanced the luminescence.

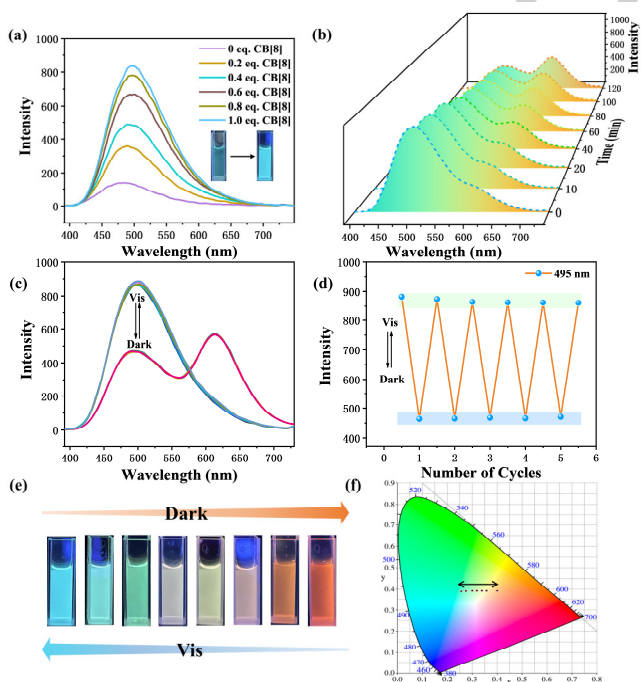


Figure 2. (a) Fluorescence spectra changes of BCNSP as the addition of 0, 0.2, 0.4, 0.6, 0.8, 1.0 eq. CB[8] in aqueous solution ($[BCNSP] = 1.0 \times 10^{-5}$ M, $[CB[8]] = 0-1.0 \times 10^{-5}$ M). (b) Fluorescence spectra changes of BCNSP \subset CB[8] with

keeping in dark. (c) Fluorescence spectra of BCNSP \subset CB[8] and of BCNMC \subset CB[8] upon alternating visible irradiation and keeping in dark. (d) Emission intensity changes at 495 nm according to (c). (e) Photographs of solutions BCNSP \subset CB[8] upon alternating visible irradiation and keeping in dark. (f) 1931 CIE chromaticity diagram of BCNSP \subset CB[8] upon alternating visible irradiation and keeping in dark ($[BCNMC] = 1.0 \times 10^{-5}$ M, $[CB[8]] = 1.0 \times 10^{-5}$ M, $\lambda_{exc} = 365$ nm).

Taking advantage of the responsiveness of spiroopyran moiety to light stimuli and acidic conditions, configuration transformation between three metastable states could be achieved under different external stimuli including light and H^+ .^[12] As shown in Figure 3a, visible light and darkness induced the guest isomerization, resulting in the ring-closed isomer BCNSP and the ring-opened isomer BCNMC, respectively. The acidic environment promoted the production of protonated isomer (BCNMCH), which was more stable, and difficult to be spontaneously isomerized under dark conditions. The fluorescence spectra further indicated the fluorescence changes between the three supramolecular systems encapsulated by different isomers (Figure 3b). Ring-opened BCNMC \subset CB[8] showed orange fluorescence attributed to two emission peaks at 495 nm and 620 nm. Protonated BCNMCH \subset CB[8] emitted blue fluorescence at about 490 nm, which was similar to that of ring-closed BCNSP \subset CB[8]. Moreover, in order to elucidate the possible mechanisms of luminescence changes of the supramolecular systems under visible light irradiation and in dark, the relationship between the UV-vis spectra of BCNSP as well as BCNMC and the fluorescence spectra of BCNSP was investigated, which found that the isomerization of spiroopyran under different irradiation conditions can lead to distinct absorption and luminescent changes. According to Figure 3c, the ring-opened BCNMC induced by dark conditions exhibited a strong absorption peak at around 370 nm and a weak one centered at 510 nm, whereas the ring-closed BCNSP induced by visible-light irradiation showed only one absorption peak at 370 nm, and that at 510 nm was negligible. As a result, the absorption spectrum of BCNMC more effectively overlapped with the fluorescence emission at 495 nm assigned to the cyanostilbene moiety of BCNSP after visible irradiation for 30 s. The overlap of the spectra indicated that the energy of the cyanostilbene and the spiroopyran functional group were matched, making it feasible for intramolecular fluorescence resonance energy transfer (FRET). On the other hand, the two functional groups were effectively brought closer to each other by alkyl chain linkage, which facilitated the realization of FRET. However, the potential fluorescence change of the guest was only clearly observed after the introduction of CB[8] to form a tight inclusion, suggesting that the necessity of effective encapsulation and confinement of the cyanostilbene moiety by the CB[8] cavity to achieve significant light-controlled luminescence behavior (Figure 3d). Subsequently, the energy transfer efficiency was calculated according to the change in fluorescence intensity before and after visible irradiation. The energy transfer efficiency of BCNSP \subset CB[8] was 59%, which was about two times higher than that of free BCNSP (32%), indicating that CB[8] not only enhanced the fluorescence of BCNSP but also increased the energy transfer efficiency between ring-closed to ring-opened conformation. In the control experiment, the spiroopyran modified by quaternary ammonium salt (SPN) and reference compound BCN4C were synthesized to explore the domain-limiting effect of the CB[8] cavities. The characteristic absorbance of SPN was at 550 nm, and the

fluorescence emission appeared at 620 nm, whose optical properties were similar to that of BCNMC (Figure S23). However, the addition of CB[8] did not enhance the red fluorescence of SPN. For BCN4C, the characteristic absorption peak at 360 nm was observed in the UV-vis absorption spectrum, and the gradual addition of CB[8] resulted in a gradual redshift of the characteristic absorption peak, which was similar to the result of CB[8] acting on BCNSP. In addition, BCN4C also exhibited a very weak fluorescence emission at 495 nm, and gradually adding CB[8] to its solution could significantly enhance the blue fluorescence with a slight blue shift (Figure S24). The obtained results indicated that the origin of the observed blue fluorescence was cyanostilbene group, and the reasons of the enhanced fluorescence was that the binding of CB[8], which further promoted the energy transfer between cyanostilbene group and the ring-opened spiropyran group under dark conditions.

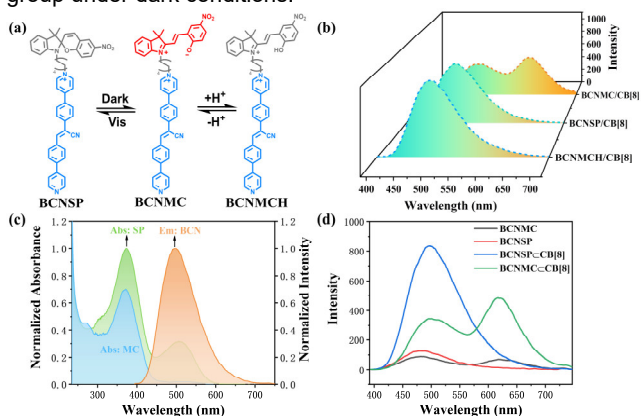


Figure 3. (a) Reversible structural transformations between three states, including BCNSP, BCNMC, and protonated BCNMCH. (b) Fluorescence spectra of different supramolecular systems of three states BCNSP \subset CB[8], BCNMC \subset CB[8] and BCNMCH \subset CB[8] ([BCNMC] = [BCNSP] = [BCNMCH] = 1.0×10^{-5} M, [CB[8]] = 1.0×10^{-5} M). (c) UV-vis spectra of ring-closed BCNSP and ring-opened BCNMC and emission spectrum of BCNSP. (d) Fluorescence spectra of BCNSP, BCNMC, BCNSP \subset CB[8], and BCNMC \subset CB[8], respectively. ([BCNMC] = [BCNSP] = 1.0×10^{-5} M, [CB[8]] = 1.0×10^{-5} M, Ex=365 nm).

Different from the unidirectional photo-response anti-counterfeiting, the bidirectional reversible BCNMC \subset CB[8] supramolecular system was successfully applied in dynamic information encryption. The fluorescent pattern with different information was fabricated through the information loading process and information decryption procedures due to the isomerization between ring-closed and ring-opened conformation (Figure 4a). The character of “NK” was obtained by irradiating the BCNMC \subset CB[8] solution in 96-well plate for 30 s upon visible light which was covered with the homemade mask. The portion exposed to visible light emitted blue fluorescence, the portion sheltered from light emitted orange fluorescence, thus the information of “NK” was observed and the information could only be read under the 365 nm UV lamp illumination, whereas no pattern could be seen or information obtained by the naked eye under room light. Subsequently, the blue fluorescent character “NK” gradually changes to green, yellow, and eventually to orange which was finally indistinguishable from the background as kept in dark, enabling the erasure of information. The time-resolved information display facilitated a higher level of security. Notably, utilizing the reversible fluorescence change property of the host-guest complex, it was possible to achieve self-erasing of patterns

in the dark and rewriting of information under visible light irradiation to sequentially obtain various secret patterns. For example, the printed pattern A (the number of “582”) had experienced the appearance under visible light irradiation and a subsequent fluorescent color change as well as eventual disappearance in dark, resulting in the reading and decryption of the message (Figure 4b). The “encryption–decryption” cycle occurred after reprinting pattern B (message “MAX” via the Morse code). In addition, a more complex color-tunable QR code was constructed. The aqueous solution of the host-guest complex was filled into the QR code model which was manufactured by 3D printing technology. After keeping it in dark for 120 min, the orange emissive QR code containing BCNMC \subset CB[8] was obtained (Figure S25). Subsequently, the color of the QR code gradually changed accompanied by a successive color change over a broad range from orange, yellow, green to blue under visible light irradiation, which completely reversed after being kept in dark. The website belonging to our group (<https://supram.nankai.edu.cn/kylw.htm>) appeared through scanning with a smartphone. Thus, the supramolecular system were capable of in situ fabricating multicolor codes, which were expected to develop into 3D color codes with high resolution through a recently reported laser direct writing technique.^[13]

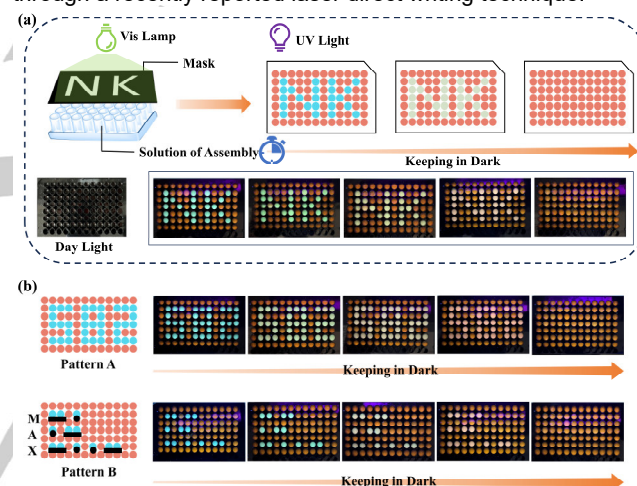


Figure 4. (a) Schematic illustration of writing processes through visible light irradiation and corresponding self-erasure of information “NK” in dark. (b) Photographs of decrypted messages of “582” over time and rewritten patterns of “MAX” via the Morse code under visible light irradiation ([BCNMC] = 3.0×10^{-5} M, [CB[8]] = 3.0×10^{-5} M).

In conclusion, we constructed a multicolor reversible supramolecular shuttle by simple host-guest complexation for dynamic information storage, which was achieved by the macrocyclic host CB[8] confined the guest spiropyran-modified cyanostilbene derivative (BCNMC) to enhance the fluorescence behavior and photoisomerization. Since the isomerization between ring-closed and ring-opened conformation of the guest, the host-guest complex changed between BCNMC \subset CB[8] and BCNSP \subset CB[8], which produced tunable multicolor fluorescence emission and reversible conversion of the topological morphology under alternating visible light irradiation on/off. Taking advantage of the optical properties, the supramolecular system was applied in writable information encryption and multicolor QR codes. Therefore, this strategy may provide a new approach for photo-

modulated reversible topological morphology conversion and multicolor bidirectional supramolecular shuttle.

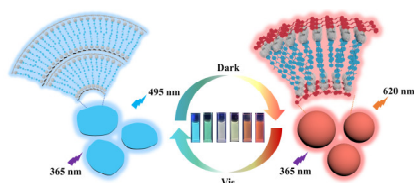
Acknowledgements

This work was financially supported by the National Natural Science Foundation of China (grant nos. 22131008 and 21971127). We thank the Fundamental Research Funds for the Central Universities and the Haihe Laboratory of Sustainable Chemical Transformations for financial support.

Keywords: supramolecular system • multicolor luminescence • photo-responsiveness • information encryption

- [1] a) Q. Qi, G. Sekhon, R. Chandradat, N. M. Ofodum, T. Shen, J. Scrimgeour, M. Joy, M. Wriedt, M. Jayathirtha, C. C. Darie, D. A. Shipp, X. Liu, X. Lu, *J. Am. Chem. Soc.* **2021**, *143*, 17337-17343; b) J.-X. Liu, K. Chen, C. Redshaw, *Chem. Soc. Rev.* **2023**, *52*, 1428-1455; c) X. Le, H. Shang, H. Yan, J. Zhang, W. Lu, M. Liu, L. Wang, G. Lu, Q. Xue, T. Chen, *Angew. Chem. Int. Ed.* **2021**, *60*, 3640-3646; d) Q. Wang, Q. Zhang, Q.-W. Zhang, X. Li, C.-X. Zhao, T.-Y. Xu, D.-H. Qu, H. Tian, *Nat. Commun.* **2020**, *11*, 158; e) Z. Li, Z. Yang, Y. Zhang, B. Yang, Y.-W. Yang, *Angew. Chem. Int. Ed.* **2022**, *61*, e202206144; f) Y. Zhang, Y. Chen, H. Zhang, L. Chen, Q. Bo, Y. Liu, *Adv. Opt. Mater.* **2023**, *11*, 2202828; g) H. Yang, S. Li, J. Zheng, G. Chen, W. Wang, Y. Miao, N. Zhu, Y. Cong, J. Fu, *Adv. Mater.* **2023**, *35*, e2301300; h) H. Zou, Y. Hai, H. Ye, L. You, *J. Am. Chem. Soc.* **2019**, *141*, 16344-16353.
- [2] a) H.-J. Yu, Q. Zhou, X. Dai, F.-F. Shen, Y.-M. Zhang, X. Xu, Y. Liu, *J. Am. Chem. Soc.* **2021**, *143*, 13887-13894; b) J. Zhang, H. Shen, X. Liu, X. Yang, S. L. Broman, H. Wang, Q. Li, J. W. Y. Lam, H. Zhang, M. Cacciarini, M. B. Nielsen, B. Z. Tang, *Angew. Chem. Int. Ed.* **2022**, *61*, e202208460; c) X. He, J. Zhang, X. Liu, Z. Jin, J. W. Y. Lam, B. Z. Tang, *Angew. Chem. Int. Ed.* **2023**, e202300353; d) J. Kim, H. Yun, Y. J. Lee, J. Lee, S.-H. Kim, K. H. Ku, B. J. Kim, *J. Am. Chem. Soc.* **2021**, *143*, 13333-13341; e) L. Wang, Q. Li, *Chem. Soc. Rev.* **2018**, *47*, 1044-1097.
- [3] a) M. Zhao, B. Li, P. Wang, L. Lu, Z. Zhang, L. Liu, S. Wang, D. Li, R. Wang, F. Zhang, *Adv. Mater.* **2018**, *30*, 1804982; b) R. Zhang, Y. Chen, L. Chen, Y. Zhang, Y. Liu, *Adv. Opt. Mater.* **2023**, 2300101; c) X.-L. Ni, S. Chen, Y. Yang, Z. Tao, *J. Am. Chem. Soc.* **2016**, *138*, 6177-6183; d) Y. Wang, H. Wu, W. Hu, J. F. Stoddart, *Adv. Mater.* **2022**, *34*, 2105405; e) W.-L. Zhou, X.-Y. Dai, W. Lin, Y. Chen, Y. Liu, *Chem. Sci.* **2023**, *14*, 6457-6466; f) H. Wu, Y. Wang, L. O. Jones, W. Liu, B. Song, Y. Cui, K. Cai, L. Zhang, D. Shen, X.-Y. Chen, Y. Jiao, C. L. Stern, X. Li, G. C. Schatz, J. F. Stoddart, *J. Am. Chem. Soc.* **2020**, *142*, 16849-16860; g) W.-L. Zhou, W. Lin, Y. Chen, X.-Y. Dai, Y. Liu, *Small.* **2023**, *19*, 2304009.
- [4] a) Z. Zheng, H. Hu, Z. Zhang, B. Liu, M. Li, D.-H. Qu, H. Tian, W.-H. Zhu, B. L. Feringa, *Nat. Photon.* **2022**, *16*, 226-234; b) J. Zhang, Y. Fu, H.-H. Han, Y. Zhang, J. Li, X.-P. He, B. L. Feringa, H. Tian, *Nat. Commun.* **2017**, *8*, 987; c) X.-F. Hou, X.-M. Chen, H. K. Bisoyi, Q. Qi, T. Xu, D. Chen, Q. Li, *ACS Appl. Mater. Inter.* **2023**, *15*, 11004-11015; d) H.-Q. Zheng, Y. Yang, Z. Wang, D. Yang, G. Qian, Y. Cui, *Adv. Mater.* **2023**, *35*, 2300177; e) R. Yang, X. Ren, L. Mei, G. Pan, X.-Z. Li, Z. Wu, S. Zhang, W. Ma, W. Yu, H.-H. Fang, C. Li, M.-Q. Zhu, Z. Hu, T. Sun, X. Bin, W. Tian, *Angew. Chem. Int. Ed.* **2022**, *61*, e202117158; f) Q. Qi, C. Li, X. Liu, S. Jiang, Z. Xu, R. Lee, M. Zhu, B. Xu, W. Tian, *J. Am. Chem. Soc.* **2017**, *139*, 16036-16039; g) P. Hong, N.-H. Xie, K. Xiong, J. Liu, M.-Q. Zhu, C. Li, *J. Mater. Chem. A.* **2023**, *11*, 5703-5713; h) E. Deniz, N. Kandoth, A. Fraix, V. Cardile, A. C. E. Graziano, D. Lo Furno, R. Gref, F. M. Raymo, S. Sortino, *Chem. Eur. J.* **2012**, *18*, 15782-15787; i) M. Yu, P. Zhang, L. Liu, H. Wang, H. Wang, C. Zhang, Y. Gao, C. Yang, J. Cui, J. Chen, *Adv. Opt. Mater.* **2021**, *9*, 2101227.
- [5] D. Kim, K. Jeong, J. E. Kwon, H. Park, S. Lee, S. Kim, S. Y. Park, *Nat. Commun.* **2019**, *10*, 3089.
- [6] X. M. Chen, W. J. Feng, H. K. Bisoyi, S. Zhang, X. Chen, H. Yang, Q. Li, *Nat. Commun.* **2022**, *13*, 3216.
- [7] H. Wu, Y. Chen, X. Dai, P. Li, J. F. Stoddart, Y. Liu, *J. Am. Chem. Soc.* **2019**, *141*, 6583-6591.
- [8] a) Z. Wang, L. Gao, Y. Zheng, Y. Zhu, Y. Zhang, X. Zheng, C. Wang, Y. Li, Y. Zhao, C. Yang, *Angew. Chem. Int. Ed.* **2022**, *61*, e202203254; b) Z. Gao, Y. Han, F. Wang, *Nat. Commun.* **2018**, *9*, 3977; c) J. Du, L. Sheng, Y. Xu, Q. Chen, C. Gu, M. Li, S. X.-A. Zhang, *Adv. Mater.* **2021**, *33*, 2008055.
- [9] a) H. Nie, Z. Wei, X.-L. Ni, Y. Liu, *Chem. Rev.* **2022**, *122*, 9032-9077. b) G. Ghale, W. M. Nau, *Acc. Chem. Res.* **2014**, *47*, 2150-2159.
- [10] S. K. Bhaumik, S. Banerjee, *ACS Appl. Mater. Inter.* **2022**, *14*, 36936-36946.
- [11] H.-J. Kim, D. R. Whang, J. Gierschner, S. Y. Park, *Angew. Chem. Int. Ed.* **2016**, *55*, 15915-15919.
- [12] P. K. Kundu, G. L. Olsen, V. Kiss, R. Klajn, *Nat. Commun.* **2014**, *5*, 3588.
- [13] a) Z. Li, H. Gao, R. Shen, C. Zhang, L. Li, Y. Lv, L. Tang, Y. Du, Q. Yuan, *Angew. Chem. Int. Ed.* **2021**, *60*, 17564-17569; b) H. Palneedi, J. H. Park, D. Maurya, M. Peddigari, G.-T. Hwang, V. Annapureddy, J.-W. Kim, J.-J. Choi, B.-D. Hahn, S. Priya, K. J. Lee, J. Ryu, *Adv. Mater.* **2018**, *30*, 1705148.

Entry for the Table of Contents



Confinement of a spiropyran-modified cyanostilbene guest (BCNMC) in a cucurbit[8]uril (CB[8]) host has led to a light-driven multicolor luminescent supramolecular shuttle, which exhibits reversible conversion of the topological morphology. Alternating irradiation with visible light and the absence of light results in different fluorescence colors for information encryption.